Electronic Supplementary Material (ESI) for Journal of Materials Chemistry C.
This journal is © The Royal Society of Chemistry 2019

SUPPORTING INFORMATION

Chemical Sensors Based on Nano-Sized Lanthanide-Grafted Periodic Mesoporous Organosilica Hybrid Materials

Anna M. Kaczmarek, and Pascal Van Der Voort**

COMOC – Center for Ordered Materials Organometallics and Catalysis, Department of Chemistry, Ghent University, Krijgslaan 281-S3, B-9000 Ghent, Belgium

Table S1 Relative Ln^{3+} contents for the PMO@Eu,Tb, PMO@Eu,Tb_phen and PMO@Eu,Tb_bpy samples from synthesis (calcd.) and as determined by XRF.

Sample	Molar amounts used in synthesis [mmol]		Eu^{3+} ion		Tb^{3+} ion	
	Eu^{3+}	Tb^{3+}	Calcd.	XRF	Calcd.	XRF
PMO@Eu,Tb	0.50	0.50	50%	48.7%	50%	51.3%
PMO@Eu,Tb_phen	0.50	0.50	50%	49.8%	50%	50.1%
PMO@Eu,Tb_bpy	0.50	0.50	50%	50.6%	50%	49.4%

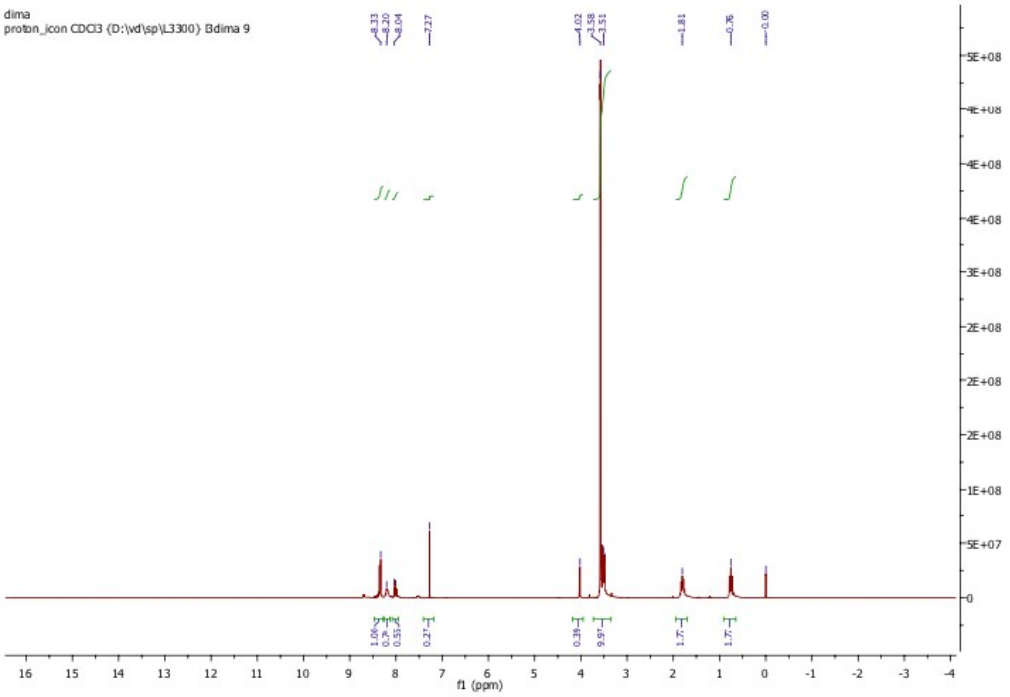

Figure S1 ^{1}H NMR of the PMO precursor ($CDCl_3$, 300 MHz).

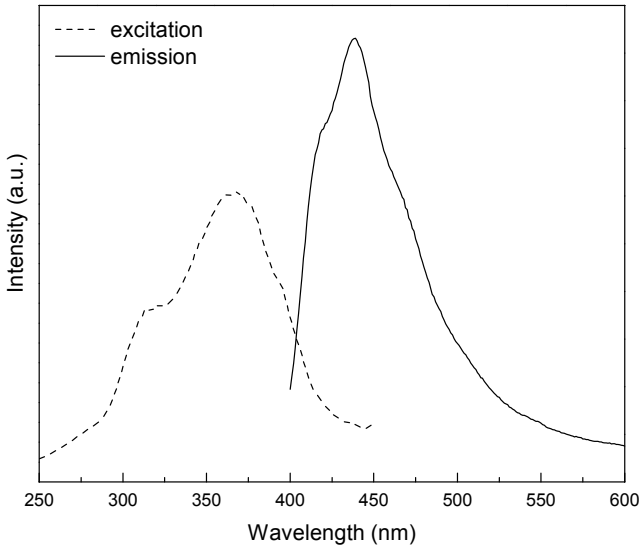

Figure S2 RT combined excitation-emission spectrum of the pristine PMO (the dotted line represents the excitation spectrum and the continuous line represents the emission spectrum).

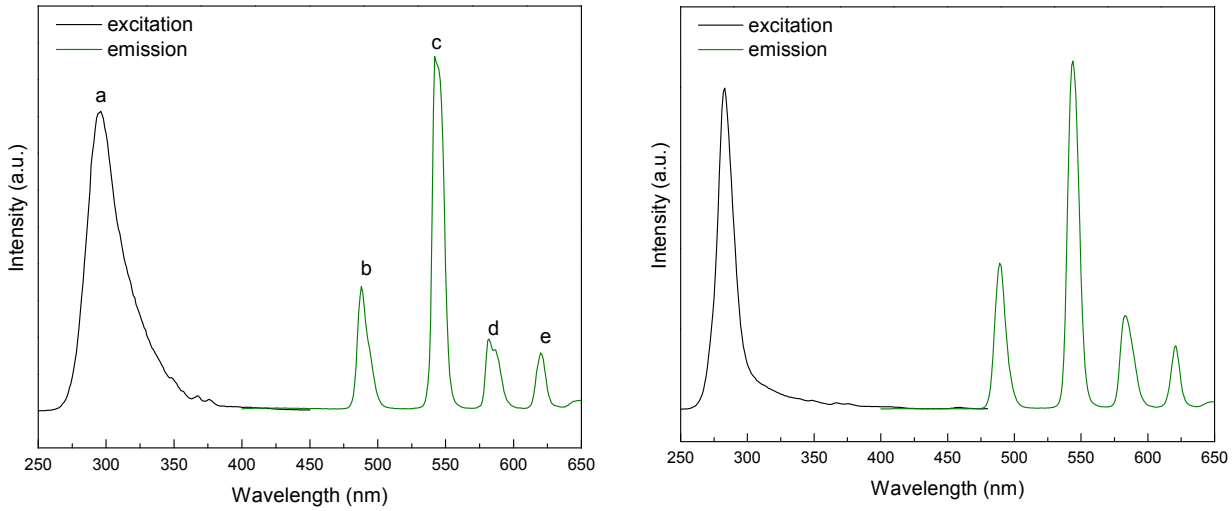

Figure S3 Left: RT solid-state combined excitation-emission spectrum of PMO@Tb, right: RT combined excitation-emission spectrum of PMO@Tb in water suspension. The emission spectra were recorded when exciting into the maximum of the broad ligand band and the excitation spectra were monitored at the $^5D_4 \rightarrow {}^7F_5$ transition peak.

Table S2 Assignment of peaks labeled in Figure S3 (PMO@Tb in solid-state).

Label	Wavelength (nm)	Transitions
	Excitation	
a	295	$\pi \rightarrow \pi^*$
	Emission	
b	488	$^5D_4 \rightarrow {}^7F_6$
c	542	$^5D_4 \rightarrow {}^7F_5$
d	581	$^5D_4 \rightarrow {}^7F_4$
e	619	$^5D_4 \rightarrow {}^7F_3$

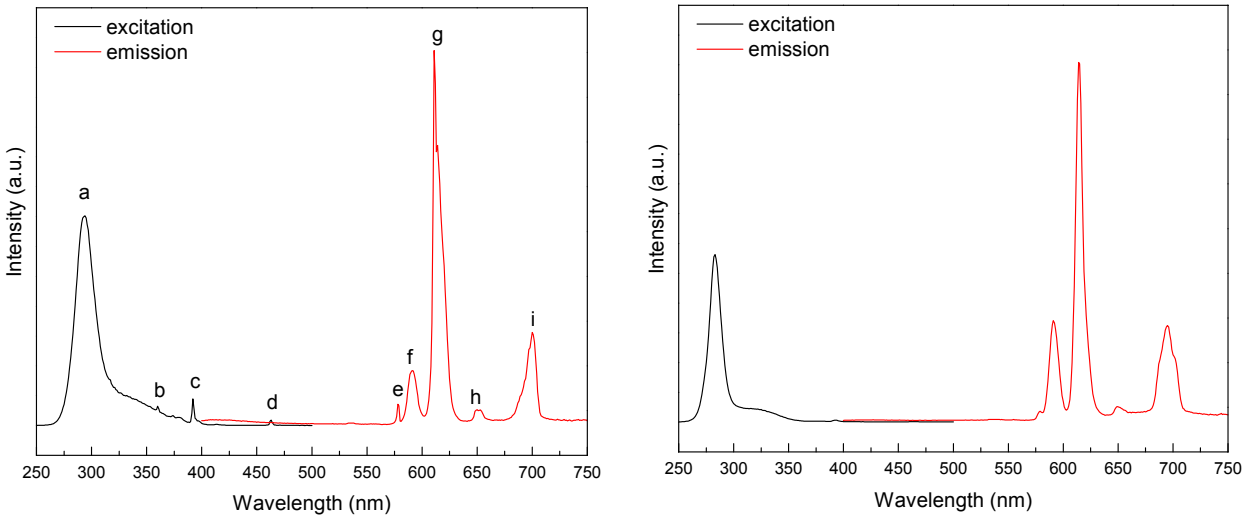

Figure S4 Left: RT solid-state combined excitation-emission spectrum of PMO@Eu, right: RT combined excitation-emission spectrum of PMO@Eu in water suspension. The emission spectra were recorded when exciting into the maximum of the broad ligand band and the excitation spectra were monitored at the $^5D_0 \rightarrow {}^7F_2$ transition peak.

Table S3 Assignment of peaks labeled in Figure S4 (PMO@Eu in solid-state).

Label	Wavelength (nm)	Transitions
	Excitation	
a	293	$\pi \rightarrow \pi^*$
b	361	$^5D_4 \leftarrow {}^7F_0$
c	392	$^5L_6 \leftarrow {}^7F_0$
d	462	$^5D_2 \leftarrow {}^7F_0$
	Emission	
e	578	$^5D_0 \rightarrow {}^7F_0$
f	591	$^5D_0 \rightarrow {}^7F_1$
g	611	$^5D_0 \rightarrow {}^7F_2$
h	651	$^5D_0 \rightarrow {}^7F_3$
i	700	$^5D_0 \rightarrow {}^7F_4$

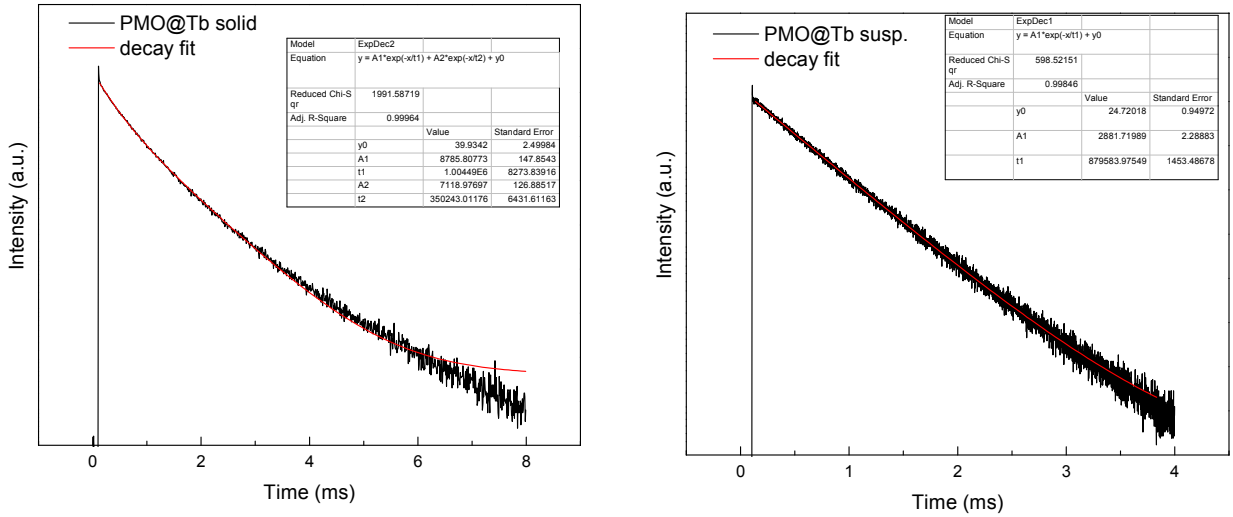

Figure S5 Left: decay profile of PMO@Tb sample in solid-state form, right: decay profile of PMO@Tb sample in suspension. The decay times were recorded when exciting into the maximum of the broad ligand band and monitoring at the $^5D_4 \rightarrow {}^7F_5$ transition peak.

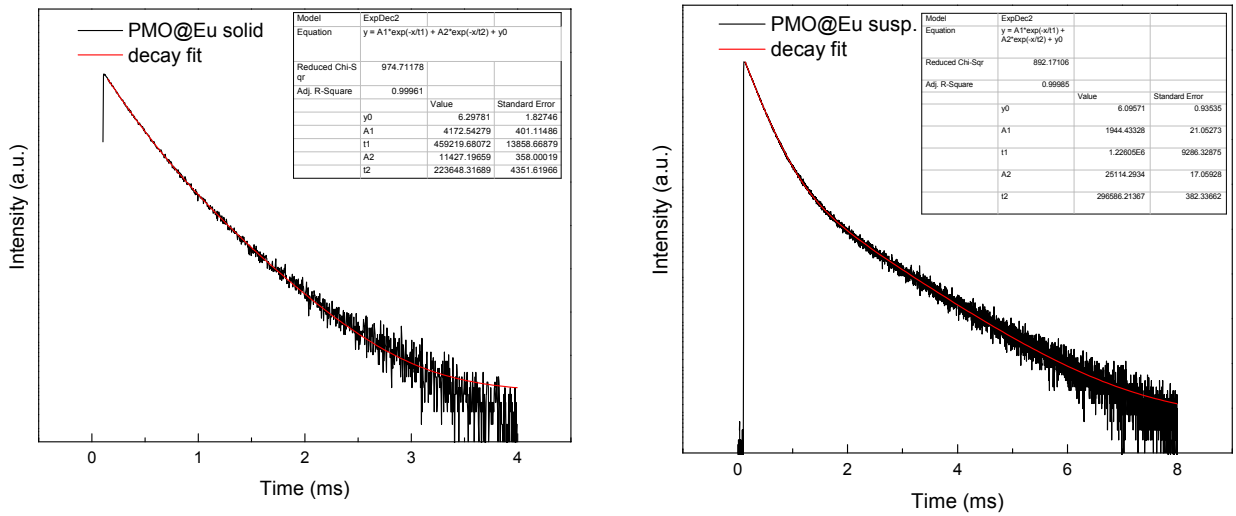

Figure S6 Left: decay profile of PMO@Eu sample in solid-state form, right: decay profile of PMO@Eu sample in suspension. The decay times were recorded when exciting into the maximum of the broad ligand band and monitoring at the $^5D_0 \rightarrow {}^7F_2$ transition peak.

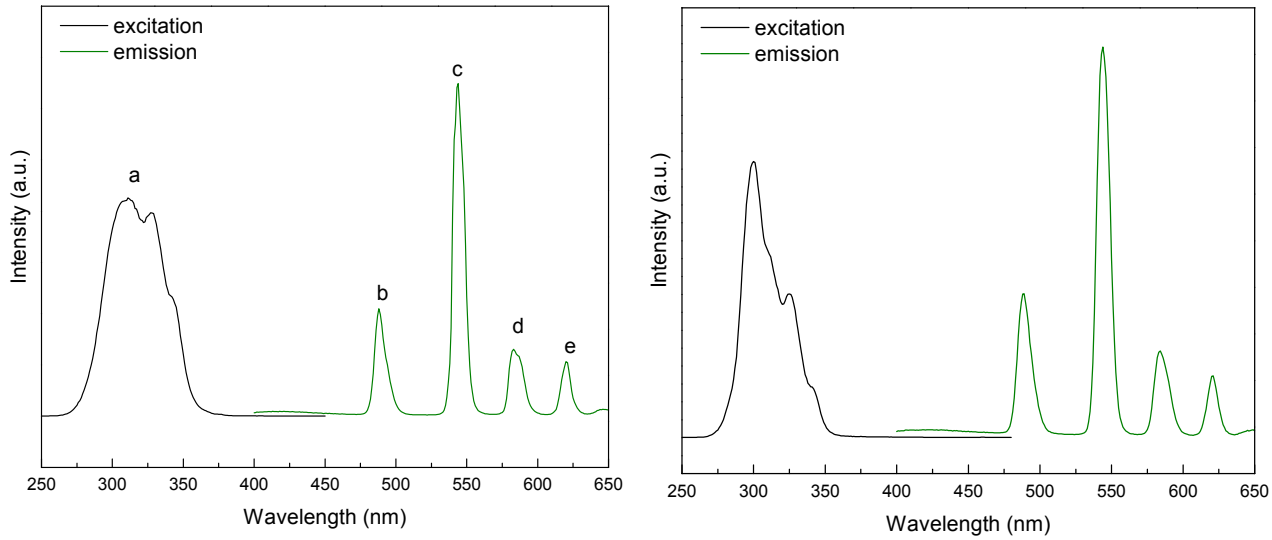

Figure S7 Left: RT solid-state combined excitation-emission spectrum of PMO@Tb_phen, right: RT combined excitation-emission spectrum of PMO@Tb_phen in water suspension. The emission spectra were recorded when exciting into the maximum of the broad ligand band and the excitation spectra were monitored at the $^5D_4 \rightarrow {}^7F_5$ transition peak.

Table S4 Assignment of peaks labeled in Figure S7 (PMO@Tb_phen in solid-state).

Label	Wavelength (nm)	Transitions
	Excitation	
a	312	$\pi \rightarrow \pi^*$
	Emission	
b	487	$^5D_4 \rightarrow {}^7F_6$
c	543	$^5D_4 \rightarrow {}^7F_5$
d	583	$^5D_4 \rightarrow {}^7F_4$

e	620	$^5D_4 \rightarrow {}^7F_3$

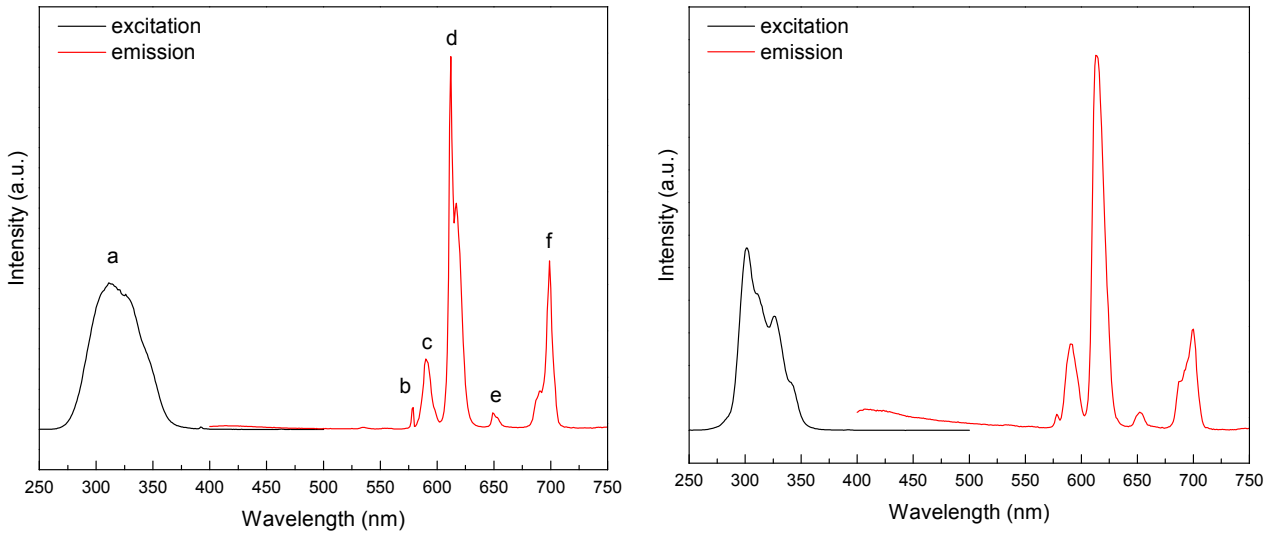

Figure S8 Left: RT solid-state combined excitation-emission spectrum of PMO@Eu_phen, right: RT combined excitation-emission spectrum of PMO@Eu_phen in water suspension. The emission spectra were recorded when exciting into the maximum of the broad ligand band and the excitation spectra were monitored at the $^5D_0 \rightarrow {}^7F_2$ transition peak.

Table S5 Assignment of peaks labeled in Figure S8 (PMO@Eu_phen in solid-state).

Label	Wavelength (nm)	Transitions
	Excitation	
a	294	$\pi \rightarrow \pi^*$
b	361	$^5D_4 \leftarrow {}^7F_0$
c	392	$^5L_6 \leftarrow {}^7F_0$
d	462	$^5D_2 \leftarrow {}^7F_0$
	Emission	
e	578	$^5D_0 \rightarrow {}^7F_0$
f	591	$^5D_0 \rightarrow {}^7F_1$
g	610	$^5D_0 \rightarrow {}^7F_2$
h	650	$^5D_0 \rightarrow {}^7F_3$
i	701	$^5D_0 \rightarrow {}^7F_4$

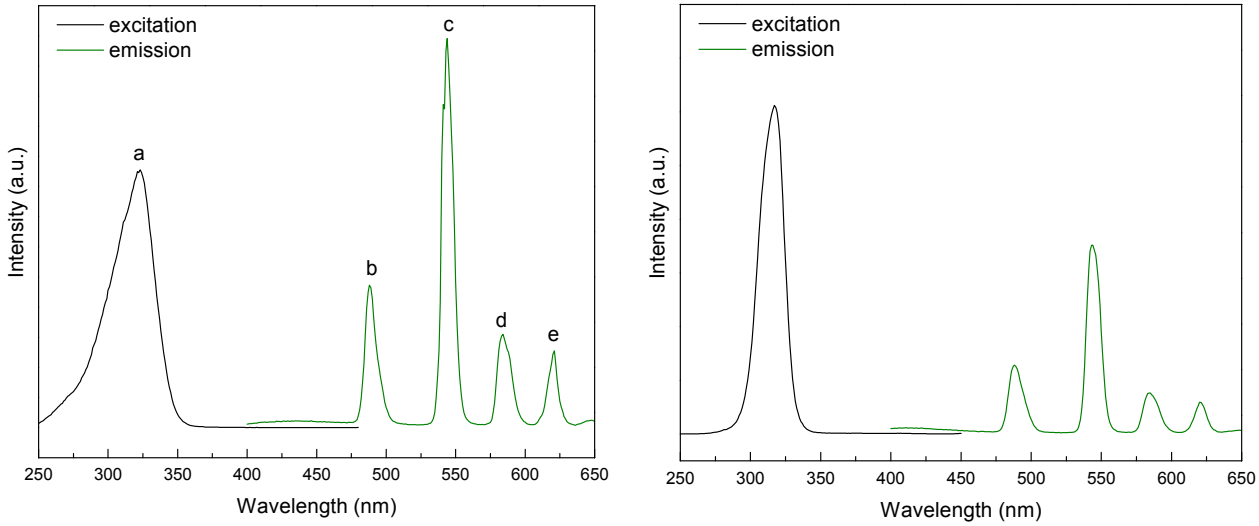

Figure S9 Left: RT solid-state combined excitation-emission spectrum of PMO@Tb_bpy, right: RT combined excitation-emission spectrum of PMO@Tb_bpy in water suspension. The emission spectra were recorded when exciting into the maximum of the broad ligand band and the excitation spectra were monitored at the $^5D_4 \rightarrow {}^7F_5$ transition peak.

Table S6 Assignment of peaks labeled in Figure S9 (PMO@Tb_bpy in solid-state).

Label	Wavelength (nm)	Transitions
	Excitation	
a	322	π→π*
	Emission	
b	489	$^5D_4 \rightarrow {}^7F_6$
c	543	$^5D_4 \rightarrow {}^7F_5$
d	583	$^5D_4 \rightarrow {}^7F_4$
e	620	$^5D_4 \rightarrow {}^7F_3$

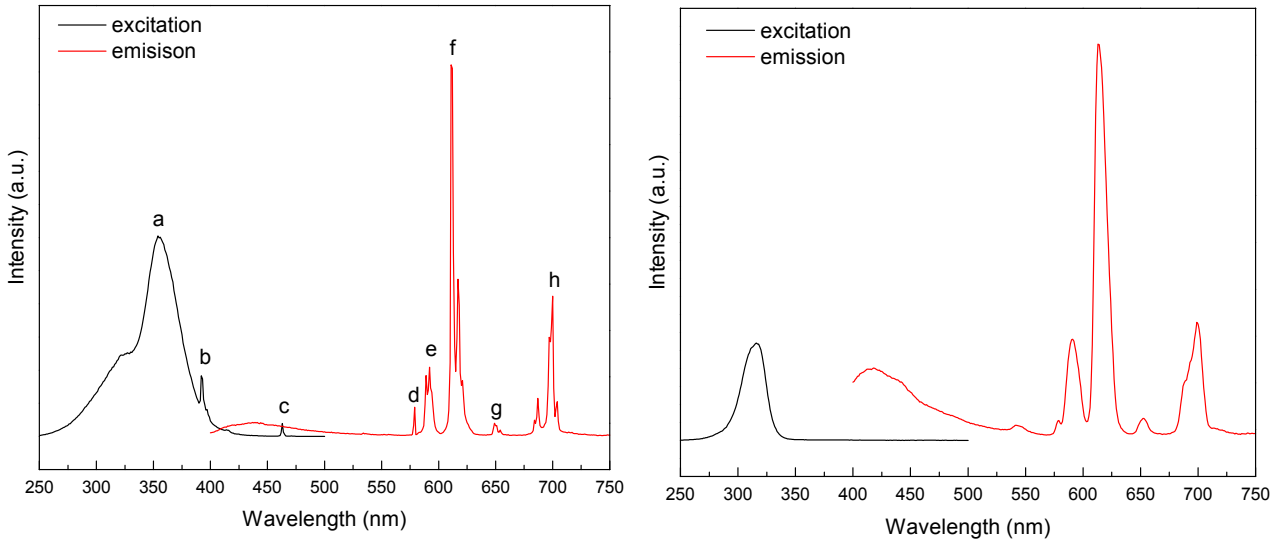

Figure S10 Left: RT solid-state combined excitation-emission spectrum of PMO@Eu_bpy, right: RT combined excitation-emission spectrum of PMO@Eu_bpy in water suspension. The emission spectra were recorded when exciting into the maximum of the broad ligand band and the excitation spectra were monitored at the $^5D_0 \rightarrow {}^7F_2$ transition peak.

Table S7 Assignment of peaks labeled in Figure S10 (PMO@Eu_bpy in solid-state).

Label	Wavelength (nm)	Transitions
	Excitation	
a	354	π→π*
b	393	$^5L_6 \leftarrow {}^7F_0$
c	462	$^5D_2 \leftarrow {}^7F_0$
	Emission	
d	579	$^5D_0 \rightarrow {}^7F_0$
e	591	$^5D_0 \rightarrow {}^7F_1$
f	612	$^5D_0 \rightarrow {}^7F_2$
g	649	$^5D_0 \rightarrow {}^7F_3$
h	698	$^5D_0 \rightarrow {}^7F_4$

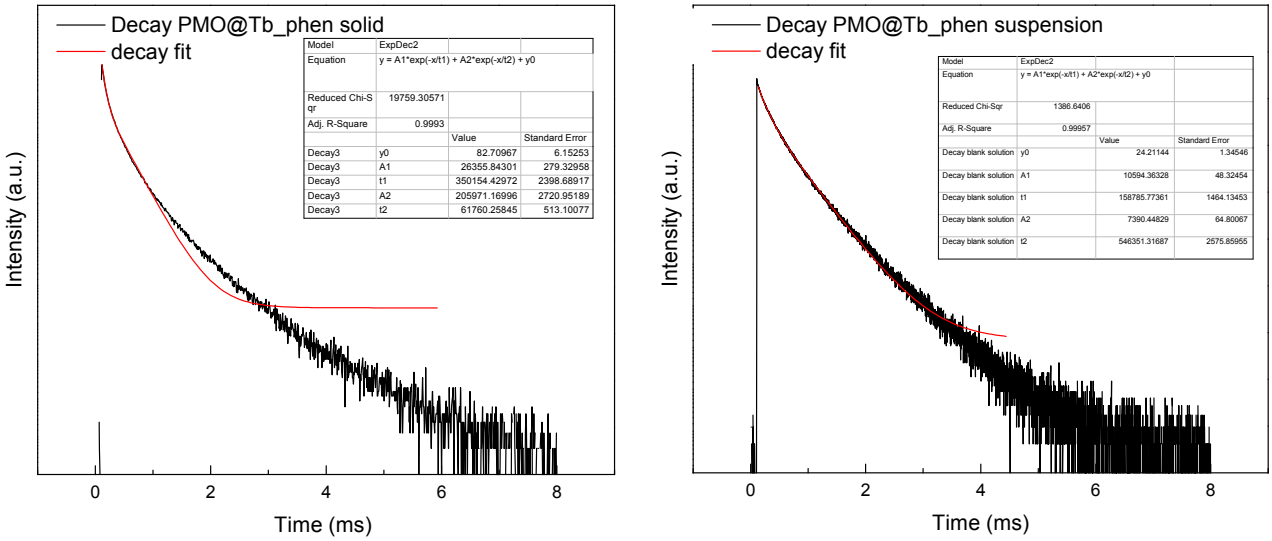

Figure S11 Left: decay profile of PMO@Tb_phen sample in solid-state form, right: decay profile of PMO@Tb_phen sample in suspension. The decay times were recorded when exciting into the maximum of the broad ligand band and monitoring at the $^5D_4 \rightarrow {}^7F_5$ transition peak.

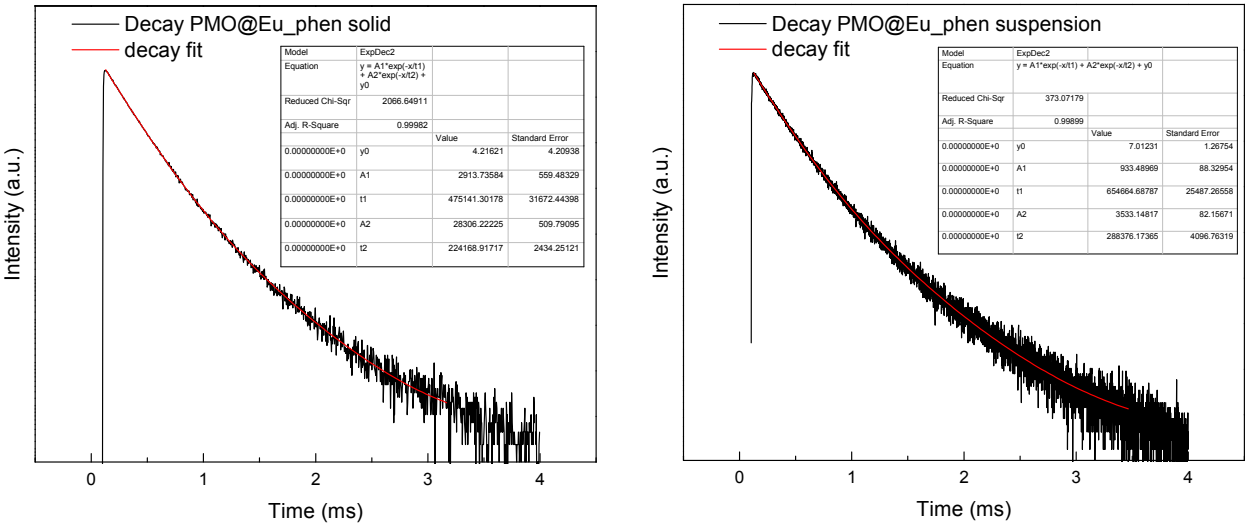

Figure S12 Left: decay profile of PMO@Eu_phen sample in solid-state form, right: decay profile of PMO@Eu_phen sample in suspension. The decay times were recorded when exciting into the maximum of the broad ligand band and monitoring at the $^5D_0 \rightarrow {}^7F_2$ transition peak.

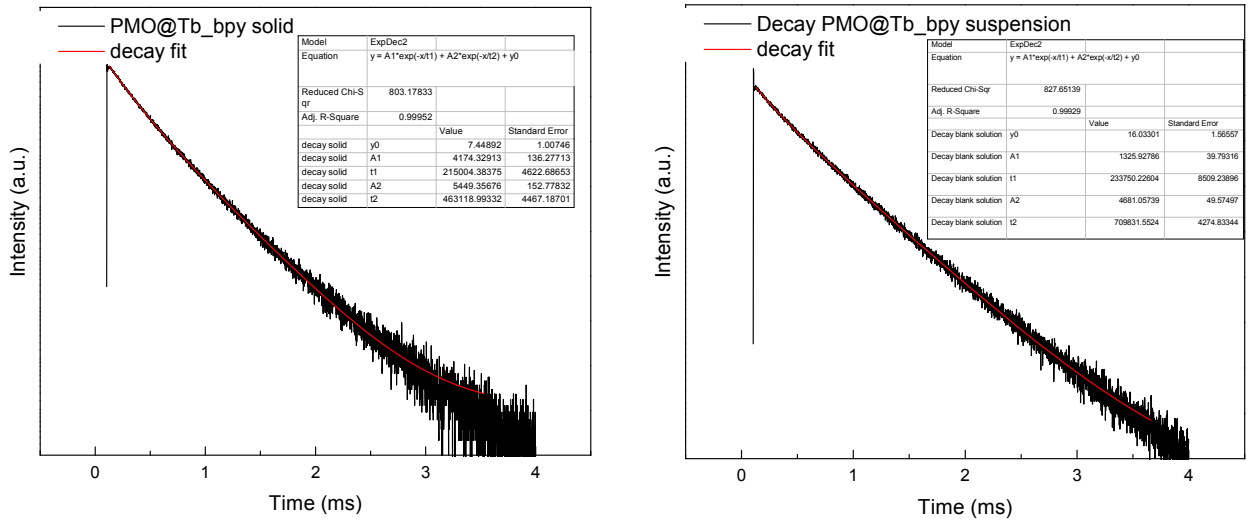

Figure S13 Left: decay profile of PMO@Tb_bpy sample in solid-state form, right: decay profile of PMO@Tb_bpy sample in suspension. The decay times were recorded when exciting into the maximum of the broad ligand band and monitoring at the $^5D_4 \rightarrow {}^7F_5$ transition peak.

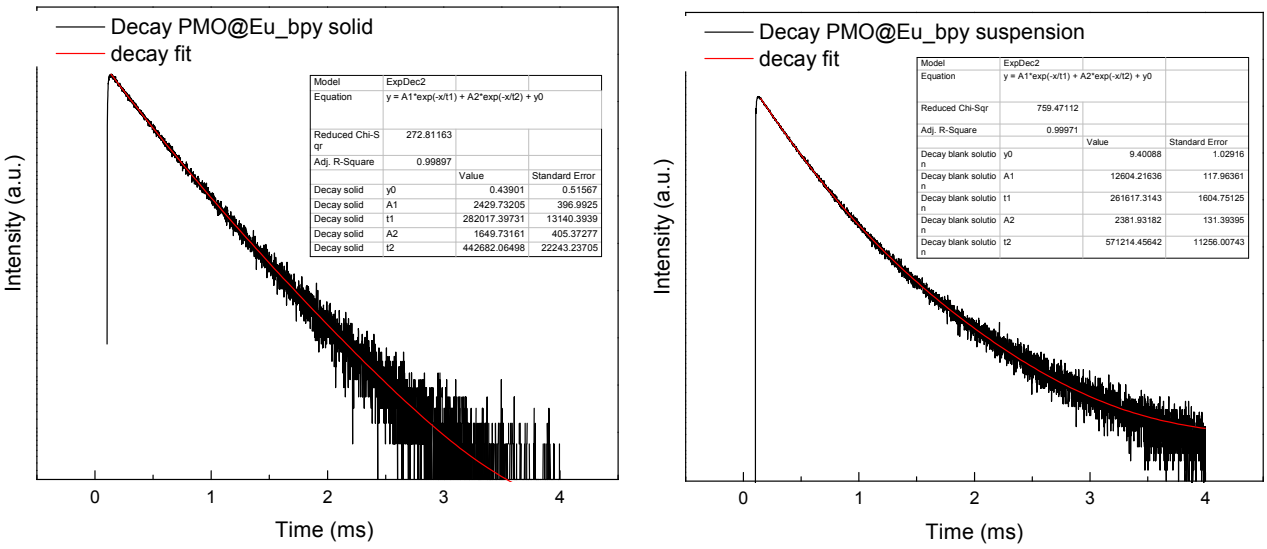

Figure S14 Left: decay profile of PMO@Eu_bpy sample in solid-state form, right: decay profile of PMO@Eu_bpy sample in suspension. The decay times were recorded when exciting into the maximum of the broad ligand band and monitoring at the $^5D_0 \rightarrow {}^7F_2$ transition peak.

Table S8 Luminescence decay times of studied materials

Sample	τ_1(μs)	τ_2 (μs)
PMO@Tb solid	1004	350
PMO@Tb suspension	879	-
PMO@Eu solid	459	224
PMO@Eu suspension	1226	296
PMO@Tb_phen	359	62
PMO@Tb_suspension	546	159
PMO@Eu_phen solid	475	224
PMO@Eu_phen suspension	654	288
PMO@Tb_bpy solid	463	215
PMO@Tb_bpy suspension	710	234
PMO@Eu_bpy solid	443	282
PMO@Eu_bpy suspension	571	262

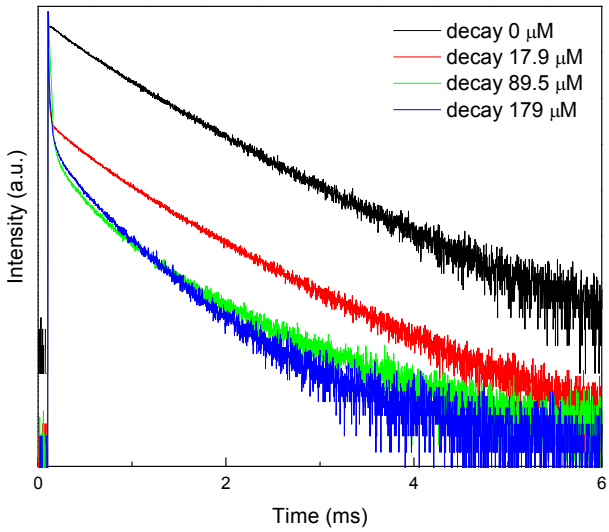

Figure S15. Luminescence decay times of PMO@Tb_bpy observed at different concentrations. A reduction in the lifetime suggests a dynamic quenching mechanism.

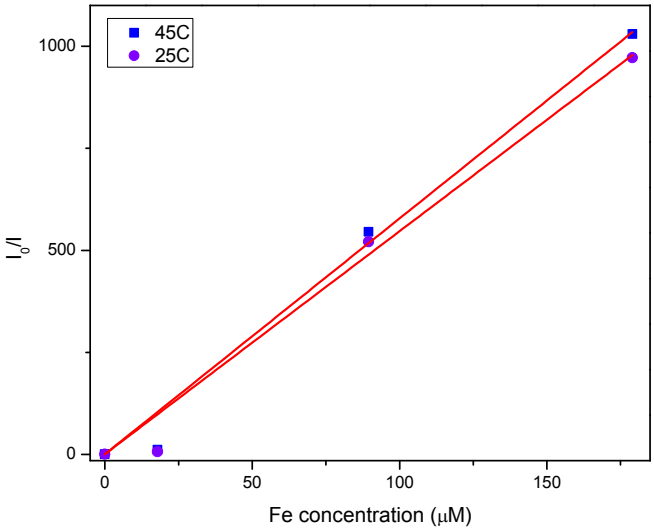

Figure S16. The Stern-Volmer curves of PMO@Tb_bpy in the presence of Fe^{2+} ions at different temperatures (25 ºC and 45 ºC).

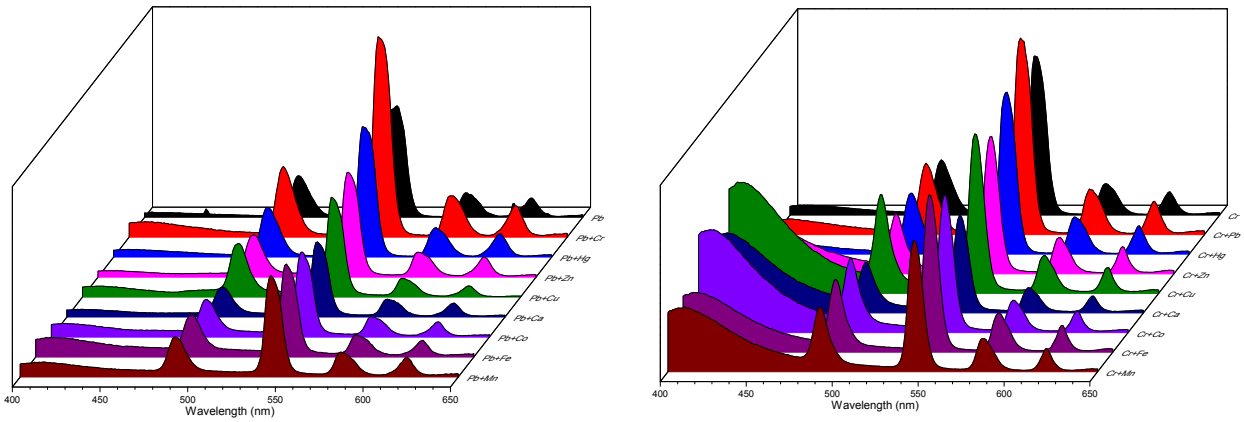

Figure S17. Emission spectra of PMO@Tb_bpy in the presence of Pb^{2+} and competing ions (left) and Cr^{3+} and competing ions (right).

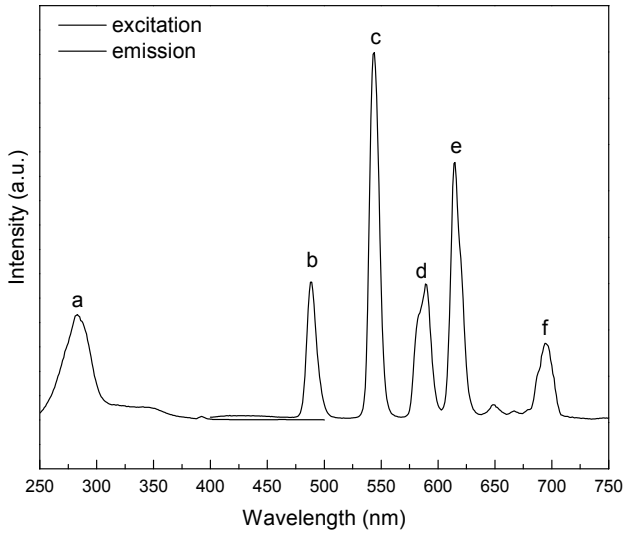

Figure S18 RT solid-state combined excitation-emission spectrum of PMO@Eu,Tb. The emission spectrum was recorded when exciting into the maximum of the broad ligand band and the excitation spectrum was monitored at the $^5D_4 \rightarrow {}^7F_5$ transition peak.

Table S9 Assignment of peaks labeled in Figure S18 (PMO@Eu,Tb in solid-state).

Label	Wavelength (nm)	Transitions
	Excitation	
a	282	$\pi \rightarrow \pi^*$
	Emission	
b	488	$^5D_4 \rightarrow {}^7F_6$ (Tb)
c	543	$^5D_4 \rightarrow {}^7F_5$ (Tb)
d	589	$^5D_0 \rightarrow {}^7F_1$ (Eu)/ $^5D_4 \rightarrow {}^7F_4$ (Tb)
e	616	$^5D_0 \rightarrow {}^7F_2$ (Eu)
f	699	$^5D_0 \rightarrow {}^7F_4$ (Eu)

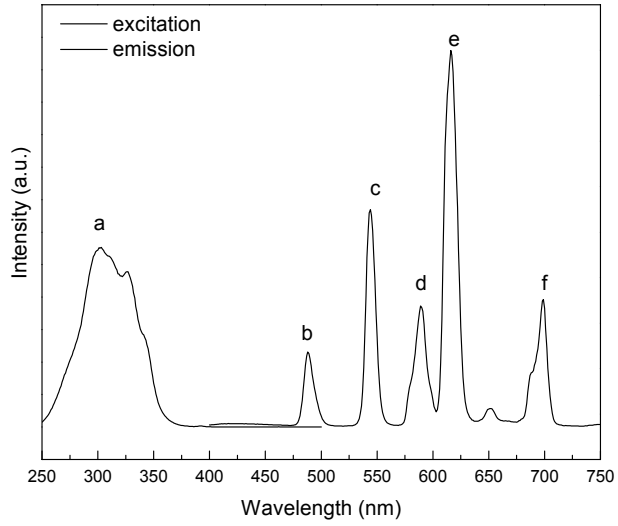

Figure S19 RT solid-state combined excitation-emission spectrum of PMO@Eu,Tb_phen. The emission spectrum was recorded when exciting into the maximum of the broad ligand band and the excitation spectrum was monitored at the $^5D_0 \rightarrow {}^7F_2$ transition peak.

Table S10 Assignment of peaks labeled in Figure S19 (PMO@Eu,Tb_phen in solid-state).

Label	Wavelength (nm)	Transitions
	Excitation	
a	300	π→π*
	Emission	
b	488	$^5D_4 \rightarrow {}^7F_6$ (Tb)
c	543	$^5D_4 \rightarrow {}^7F_5$ (Tb)
d	588	$^5D_0 \rightarrow {}^7F_1$ (Eu)/ $^5D_4 \rightarrow {}^7F_4$ (Tb)
e	616	$^5D_0 \rightarrow {}^7F_2$ (Eu)
f	698	$^5D_0 \rightarrow {}^7F_4$ (Eu)

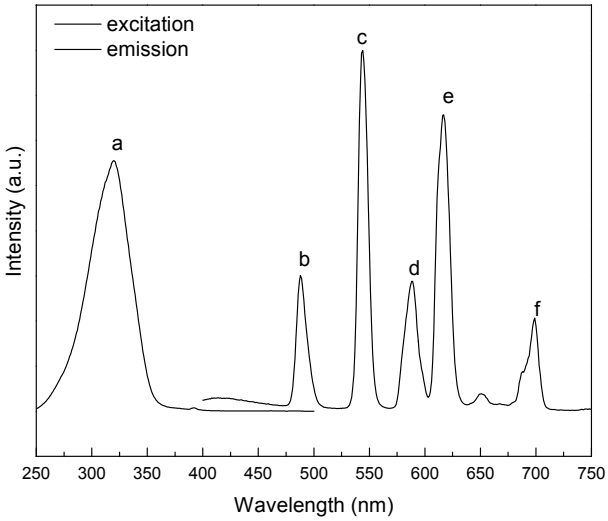

Figure S20 RT solid-state combined excitation-emission spectrum of PMO@Eu,Tb_bpy. The emission spectrum was recorded when exciting into the maximum of the broad ligand band and the excitation spectrum was monitored at the $^5D_4 \rightarrow {}^7F_5$ transition peak.

Table S11 Assignment of peaks labeled in Figure S20 (PMO@Eu,Tb_bpy in solid-state).

Label	Wavelength (nm)	Transitions
	Excitation	
a	319	π→π*
	Emission	
b	488	$^5D_4 \rightarrow {}^7F_6$ (Tb)
c	544	$^5D_4 \rightarrow {}^7F_5$ (Tb)
d	589	$^5D_0 \rightarrow {}^7F_1$ (Eu)/ $^5D_4 \rightarrow {}^7F_4$ (Tb)
e	617	$^5D_0 \rightarrow {}^7F_2$ (Eu)
f	700	$^5D_0 \rightarrow {}^7F_4$ (Eu)

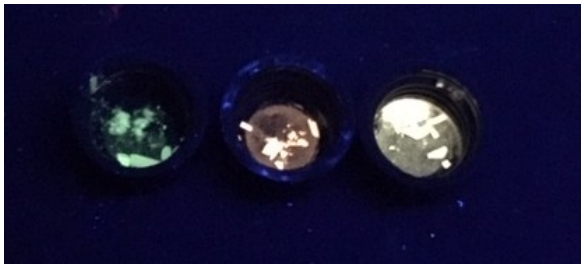

Figure S21 Photo taken under the UV lamp (302 nm excitation) of the PMO@Eu,Tb (left), PMO@Eu,Tb_phen (center) and PMO@Eu,Tb_bpy (left) samples.

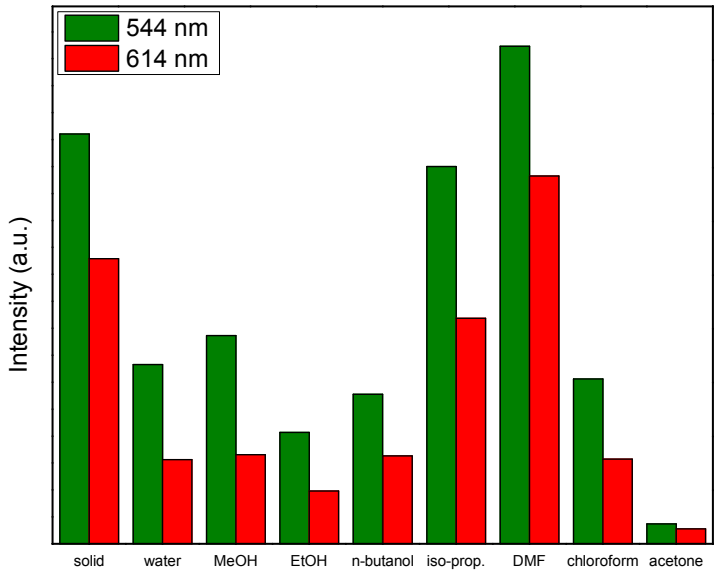

Figure S22 Bar graph representing the ratio of the 544 nm and 614 nm emission peaks in the PMO@Eu,Tb material dispersed in different solvents.

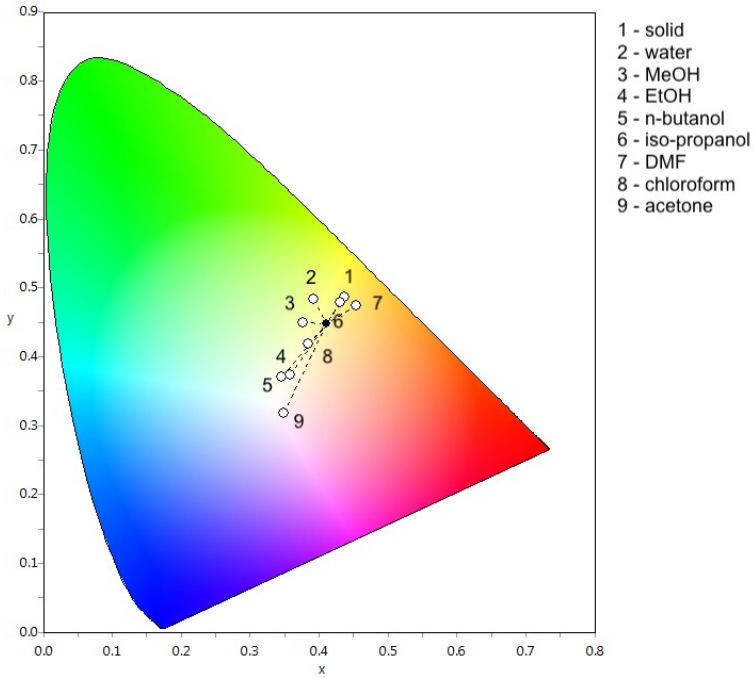

Figure S23 CIE color diagram showing the color change for PMO@Eu,Tb when dispersed in different solvents.

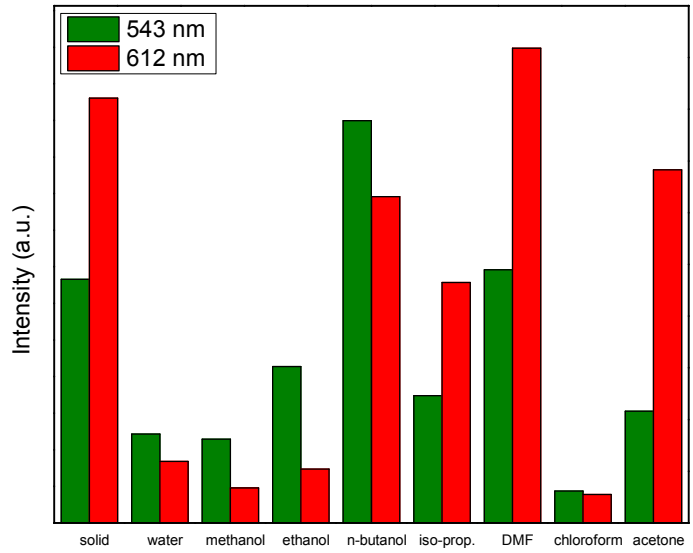

Figure S24 Bar graph representing the ratio of the 543 nm and 612 nm emission peaks in the PMO@Eu,Tb_phen material dispersed in different solvents.

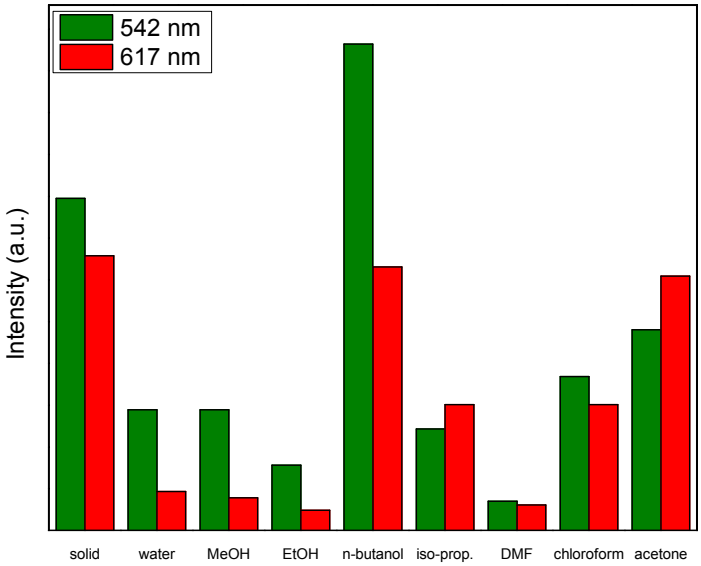

Figure S25 Bar graph representing the ratio of the 542 nm and 617 nm emission peaks in the PMO@Eu,Tb_bpy material dispersed in different solvents.